

## Anisotropy studies of ultrafast dipole reorientations

R M HOCHSTRASSER\*, M A PEREIRA, P E SHARE,  
M J SARISKY, Y R KIM, S T REPINEC, R J SENSION,  
J R G THORNE, M IANNONE, R DILLER, P A ANFINRUD,  
C HAN, T LIAN and B LOCKE

Department of Chemistry, University of Pennsylvania, Philadelphia, PA 19104 – 6323, USA

**Abstract.** Various ways in which the anisotropy can be used to understand ultrafast processes are presented and discussed. Examples include molecular reorientation, energy transfer between identical systems, excitation dynamics in polymers, reactant product alignment, protein dynamics and internal motions in fluxional molecules.

**Keywords.** Ultrafast; femtosecond lasers; anisotropy.

### 1. Introduction

Quite frequently in chemical dynamic and spectroscopic measurements on isotropic systems the use of polarized light permits observations of phenomena that cannot be studied if isotropy of the system is maintained during the experiment. For example, overall molecular rotation and the transfer of atoms (e.g. protons), electrons or excitations between identical systems might all show time dependent changes in anisotropy but not in the spectra of the various populations. Also measurements of anisotropy during a chemical reaction may yield information on the alignment of reactants and products which provides additional information on the reaction coordinate. A number of such examples will be discussed in this paper.

In a two-photon (or four-wave) experiment the signal  $S_{\parallel}(\tau)$  from a pump/probe configuration in which both pump and probe pulses, separated by time  $\tau$  have the same polarization differs in general from that with them perpendicular,  $S_{\perp}(\tau)$ , by an amount  $r_0(\tau)S(\tau)$  where  $S(\tau)$  is the omnidirectional signal,  $S_{\parallel}(\tau) + 2S_{\perp}(\tau)$ , and  $r_0(\tau)$  is defined as the anisotropy observed at time  $\tau$  after pumping. In practice, samples are pumped with pulses having finite time width so that  $r_0(\tau)$  is the anisotropy *observed* for a time delay  $\tau$  between the pump and probe pulses. Obviously if  $\tau$  is sufficiently large the system again becomes isotropic: i.e.,  $r_0(\tau) \rightarrow 0$  as  $\tau \rightarrow \infty$ . If both pump and probe pulses were infinitesimally short, or at the least much shorter than any dynamical phenomena of interest, we would obtain the *anisotropy response*  $r(t)$  in which it is assumed that the pump occurs at  $t = 0$ . Often,  $r(t)$  can be obtained from  $r_0(\tau)$  by straightforward deconvolution procedures.

The anisotropy  $r(t)$  depends in a simple way on the geometrical relationship between the pumped and probed transition dipoles: The specific nature and spatial location

---

\* For correspondence

of these dipoles is irrelevant so there are many different physical processes that can generate an anisotropy. Some of these are discussed briefly later. Many papers have been written on the interpretation of  $r(t)$ , most of them having been concerned with fluorescence polarization (Berne and Pecora 1976; Szabo 1984). The basic structure of  $r(t)$  is readily seen, however, from a very simple argument: If  $|\mathbf{Z} \cdot \hat{\mu}_1|^2 = Z_1^2$  corresponds to the squared projection of a Z-polarized electromagnetic field onto a molecule fixed axis determining the pumping step and  $Z_2^2$  is the same quantity for the probe step (note that  $Z_2^2$  would be different at each instant if some motion of the system were occurring) then:

$$S_{\parallel} = c \cdot \langle Z_1^2 Z_2^2 \rangle,$$

and

$$S_{\perp} = c \cdot \langle Z_1^2 X_2^2 \rangle = \frac{c}{2} \langle Z_1^2 (X_2^2 + Y_2^2) \rangle = \frac{c}{2} \langle Z_1^2 (1 - Z_2^2) \rangle,$$

where  $\langle \dots \rangle$  means average over the appropriate probability distribution of angles and  $c$  is an instrumental constant. The last step arises because on the average it makes no difference whether  $X$  or  $Y$  polarization is used to determine  $S_{\perp}$ . Clearly  $S_{\parallel} + 2S_{\perp} = c/3$ , since  $\langle Z_1^2 \rangle = 1/3$ . Substitution of

$$\cos^2 \theta = \frac{1}{3} [1 + 2P_2(\cos \theta)],$$

and recalling that  $\langle P_2(\cos \theta) \rangle = 0$ , if the average is over a uniform angular distribution, yields:

$$\frac{S_{\parallel} - S_{\perp}}{S_{\parallel} + 2S_{\perp}} = r(t) = 2 \langle P_2[Z_1] P_2[Z_2] \rangle.$$

This result is further simplified by recognizing that  $\langle P_2[Z_1] P_2[Z_2] \rangle = \langle P_2[Z_1] P_2[Z_1] P_2[\hat{\mu}_1 \cdot \hat{\mu}_2] \rangle$ . The angle between  $\hat{\mu}_1$  and  $\hat{\mu}_2$  is statistically independent of  $Z_1$  so with  $\langle P_2^2[Z_1] \rangle = 1/5$  (by integration over a uniform distribution of angles) it is found that:

$$r(t) = \frac{2}{5} \langle P_2[\hat{\mu}_1(0) \cdot \hat{\mu}_2(t)] \rangle, \quad (1)$$

where the times are now mentioned explicitly and  $\hat{\mu}_1$  and  $\hat{\mu}_2$  are the relevant dipole directions associated with the first and second steps. Since  $-\frac{1}{2} \leq P_2(\cos \theta) \leq 1$  the anisotropy has a minimum value of  $-0.2$  and a maximum of  $0.4$  for a one-component system.

The evaluation of the correlation function  $\langle P_2[\hat{\mu}(0) \cdot \hat{\mu}(t)] \rangle$  requires knowledge of the initial, usually equilibrium, distribution of orientations and the probability that some other specific orientation be reached from it by time  $t$ . This latter conditional probability distribution might result from free rotation, vibration or libration in which case it has a sharp value at each time as predicted by the appropriate inertial equations of motion (trajectories). On the other hand, the new orientations may also involve a diffusive process so that a broader distribution of orientations could result from a specific initial condition. In this case a diffusion equation needs to be solved to obtain the conditional distribution. Another example occurs when an equilibrium distribution of reactants is converted to chemical products. The conditional distribution

in this example must describe the reaction pathways on the potential surface in addition to the diffusive or reactive motions mentioned previously.

## 2. Overall rotational dynamics of molecules

The subject of rotational dynamics is an old one that has been thoroughly treated theoretically (Berne and Pecora 1976). The solvent friction responsible for the dissipation of rotational energy of solute molecules relates to the macroscopic solvent viscosity through Stokes law. In cases where the solvent is represented by a continuum, the Stokes–Einstein–Debye prediction for the overall rotational diffusion time  $\tau_R$  ( $\tau_R = \eta V/k_B T$ ) is very useful. This continuum limit appears to have validity when the solute molecules are very large compared with those of the solvent. The opposite limit of small or comparably sized solvent molecules is not so well understood. It is at this limit where one expects to require some details of the intermolecular potentials in order to predict the dynamics. Also in this limit the solute rotational motion is not expected to be diffusive since if the friction is inefficient, the rotational energy of the solute will not be so effectively dissipated and inertial-like motions of the solute will occur.

Inertial (essentially free) rotations can be studied with picosecond or subpicosecond techniques. The mean rotational period for a molecule having moment of inertia  $I$  is approximately  $(I/kT)^{1/2}$ . For molecules the size of benzene the mean inertial period is  $\approx 500$  fs and such motions are readily observable in gases (Myers *et al* 1986). We have recently examined the rotational dynamics of aniline in various solvents (Myers *et al* 1987; Pereira *et al* 1991) and discovered that in this case there is a significant free motion component. These measurements, made possible by femtosecond laser methods, are shown in figure 1 from Pereira *et al* (1991). The intensities of fluorescence polarized parallel and perpendicular to the exciting radiation were measured and used to calculate the fluorescence anisotropy plotted in the figure. The results are not predicted by hydrodynamic models involving macroscopic viscosity nor are they consistent with aniline being a free rotor. The “in-between” situation is one where the aniline molecule makes rather large quasi-inertial excursions ( $\approx 25^\circ$ ) between collisions with solvent that reorient the molecule and cause changes in its rotational energy. The extended diffusion theory of Gordon (1966) which incorporates this type of physics requires specification of a collisional frequency of  $\approx 200$  fs for this case. In

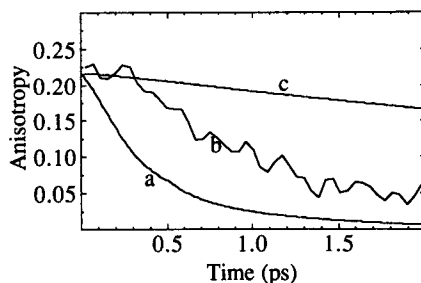


**Figure 1.** Fluorescence anisotropy of aniline in isopentane: (a) Calculation based on stick hydrodynamics, (b) Experimental result and (c) Calculation based on slip hydrodynamics.

the present case the Enskog frequencies for the series isopentane, hexane, hexadecane correlated badly with those required to fit the extended diffusion theory to the data (Pereira *et al* 1991). Since analytical theory does not easily predict this result, it is natural to turn to molecular dynamics simulations.

### 3. Energy transfer between identical systems

The anisotropy is specially useful in detecting motions of atoms or excitations between systems that are the same (and therefore have the same spectra) except for their orientation in the laboratory frame. Imagine, as in figure 2, two identical molecules a and b one of which is excited. The two possible excited states ( $a^*b$  and  $ab^*$ ) have a coupling energy  $\hbar\beta$ . If at  $t = 0$  the excitation is on the a-part and the molecule is isolated, the excitation will oscillate back and forth between a and b with the period  $2\pi/\beta$  and the instantaneous transition dipole at time  $\tau$  is  $\hat{\mu}(t) = \hat{\mu}_a \cos \beta t + i\hat{\mu}_b \sin \beta t$ . The anisotropy is therefore given by:

$$r(t) = \frac{2}{5} P_2 [\hat{\mu}_a(0) \cdot \hat{\mu}(t)] = \frac{2}{5} [\cos^2 \beta t + P_2(\cos \theta) \sin^2 \beta t], \quad (2)$$

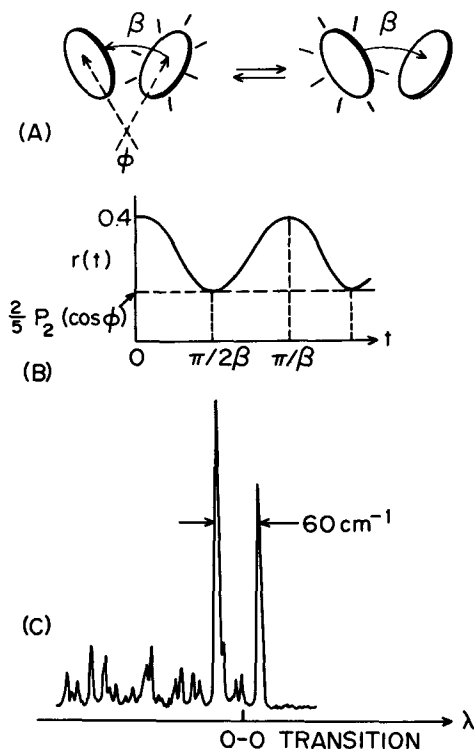


**Figure 2.** Time dependence of energy transfer: (A) model system; (B) theoretical time dependence of the dimer anisotropy; (c) spectrum of the dimer.

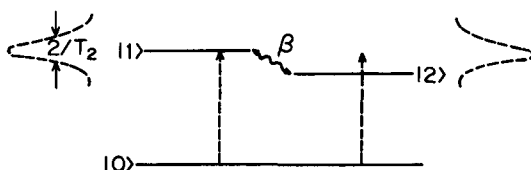


**Figure 3.** Level diagram at some instant of dimer levels when each component energy is subject to uncorrelated random fluctuation due to interactions with the surroundings. The  $0 \rightarrow 1$  and  $0 \rightarrow 2$  spectral widths are  $2/T_2$ .

where  $\cos\theta = \hat{\mu}_a \cdot \hat{\mu}_b$ . It would be straightforward to directly observe this anisotropy oscillation in a time domain experiment by exciting with a pulse shorter than  $\approx 2\pi/\beta$ , but of course for a homogeneous sample the result is entirely equivalent to the occurrence of two spectral lines separated by an energy  $2\hbar\beta$ . In fact this is what is seen in the case of bifluorene studied by Topp and coworkers (Motyka *et al* 1991) in a supersonic jet (see inset in figure 2). In this example the lines are separated by  $\beta/\pi c_0 = 60 \text{ cm}^{-1}$ . A pulse shorter than  $\approx 360 \text{ fs}$  is needed to see the beating. Of much greater interest is what occurs when such a system is in the condensed phase.

The collisions with surrounding molecules causes the parts a and b of the molecule to be inequivalent at each instant but equivalent on average. The situation is now as shown in figure 3 which corresponds to the level diagram at one instant  $t$ . The excited states of a and b are not degenerate and transitions to each of them are characterized by a dephasing time  $T_2$ . The relative magnitudes of  $T_2$  and  $1/\beta$  determine whether or not the system can oscillate as in figure 2 or die out after one-half cycle. A simple phenomenological treatment of this problem (Kim *et al* 1989) leads to the following equations of motion for the sum  $S(t)$  and difference  $\Delta(t)$  between the populations in a and b states:

$$\dot{S}(t) = -S(t)/T_1, \quad (3)$$

$$\ddot{\Delta}(t) + \left(\frac{1}{T_1} + \frac{2}{T_2}\right)\dot{\Delta}(t) + \left(4\beta^2 + \frac{2}{T_1 T_2}\right)\Delta(t) = 0. \quad (4)$$

Note that if the dephasing time is very short compared with all other times in the problem, the equation for  $\Delta(t)$  reduces to:

$$\dot{\Delta}(t) = -\Delta(t) \left[ 2\gamma + \frac{1}{T_1} \right], \quad (5)$$

where  $\gamma = \beta^2 T_2$ . This result of (5) is precisely what would be obtained if ordinary kinetics were used to calculate the difference in populations between two states each disappearing with rate coefficients  $1/T_1$  and interchanging with rate coefficient  $\gamma$ . The solution when a is the initially formed state is an exponential decay to the equilibrium ( $\Delta = 0$  in this case) value of  $\Delta$ . The anisotropy is readily shown to be given by

$$r(t) = r_{\text{eq}} + \Delta(t) \{r_a(t) - \langle P_2(\cos\theta) \rangle r_b(t)\} / 2S(t). \quad (6)$$

This takes a particularly simple form when the motion of the excitation is overdamped

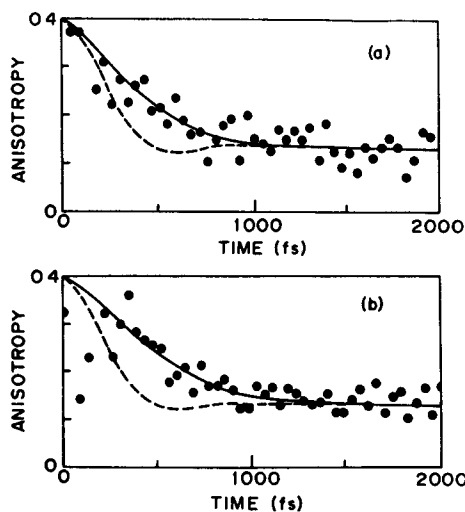


**Figure 4.** Experimental femtosecond anisotropy data for bifluorene and corresponding calculated fits using method described in the text: (a) pentanol:  $T_2 = 70$  fs (solid curve);  $T_2 = 200$  fs (dashed curve); (b) decanol:  $T_2 = 54$  fs (solid curve);  $T_2 = 200$  fs (dashed curve).

(i.e.  $1/T_2 \gg \beta$ ):

$$r(t) = \frac{1}{5} e^{-t/\tau_{\text{ROT}}} \{ [1 + \langle P_2(\cos\theta) \rangle] + [1 - \langle P_2(\cos\theta) \rangle] e^{-2\gamma t} \}. \quad (7)$$

In these expressions  $r_a(t)$  and  $r_b(t)$  are the anisotropies expected for a and b independently,  $r_{\text{eq}}$  is the anisotropy approached as  $\Delta \rightarrow 0$  if there were no overall motion and  $\tau_{\text{ROT}}$  is the overall rotational diffusion time for the system of the two coupled molecules.

The experiments on bifluorene required measurement of the subpicosecond anisotropy changes to show (see figure 4) that the excitation was overdamped and (7) was the appropriate description. The best value of  $\gamma$  fitting these data was 600 fs corresponding to  $T_2 = 60 \pm 20$  fs. The experiment also provides the value of  $P_2(\cos\theta)$  leading to  $\theta \sim 80^\circ$  somewhat dependent on the solvent.

#### 4. Excitation dynamics in polymers

Another example of anisotropy exposing dynamics that is not seen by population measurements concerns spatial excitation transport in polymers. For example, when a linear chain polymer such as polydiacetylene or polysilane is excited to its exciton band, the spatial extent of the excitation is finite. The excitation then may migrate along the chain as a result of coupling between these finite regions (Kim *et al* 1988; Thorne *et al* 1990). If the polymer is extended in one dimension (i.e. straight) these excitation dynamics will not cause a change in the anisotropy. However, if the chain is twisted, the migration of excitation will lead to a change in the orientation of the transition dipole with respect to the laboratory axes. Again, the anisotropy is given

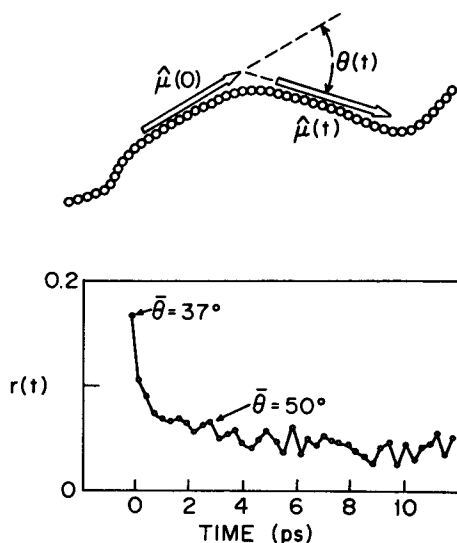


**Figure 5.** Energy transfer anisotropy in polymers. (a) Cartoon of 1-D chain polymer. Excitation is in one region while later the excitation may have changed its spatial location hence reorienting the transition dipole. (b) Results of absorption anisotropy in poly di-*n*-hexylsilane.

by (1) where now  $\hat{\mu}_1$  and  $\hat{\mu}_2$  are the exciton transition dipoles at two different times. To evaluate this correlation function neglecting the slow overall motion of the polymer in the laboratory frame, we require the probability that the transition dipole will have rotated through an angle  $\theta$  by time  $t$ . This process is depicted in figure 5 and is shown with a recent experimental result for the fluorescence anisotropy of a polysilane (Thorne *et al* 1990). The average angle of rotation of the transition dipole can be estimated by assuming all angles within a cone with semi angle  $\bar{\theta}(t)$  are equally probable at time  $t$  so that:

$$r(t)/r(0) = \frac{1}{2} \int_0^{\bar{\theta}} d(\cos \theta) [3 \cos^2 \theta - 1] / \int_0^{\bar{\theta}} d(\cos \theta). \quad (8)$$

Thus the highest anisotropy observed with a system having instrument function of 300 fs of 0.17 corresponds to  $\bar{\theta} = 37^\circ$  and by 2–3 ps we find  $\bar{\theta} \approx 50$ . In this example, like the previous one, we can watch the excitations transport along the chains even though the spectra do not change significantly with time.

## 5. Reactant product alignment

Anisotropy measurements can contribute toward understanding reaction dynamics by providing knowledge of the alignment of transition dipoles in the reactants and products. This concept was widely used in gas phase reactions but was only recently applied to condensed phases (Abrash *et al* 1990). The example concerned the isomerism of *cis*-stilbene induced by a UV femtosecond pulse. *Trans*-stilbene and dihydro-

phentaene products are formed (Wisnonski-Knittel *et al* 1974; Saltiel and Sun 1990) in this reaction. The orientation of the transition dipoles (ground to first excited state) of each of these species relative to that of *cis*-stilbene can be measured by probing their absorption with polarized femtosecond pulses following the photoinitiation of the reaction.

The *trans*-stilbene transition dipole is along the longest axis of the molecule and so has the molecule fixed vector:  $\hat{\mu}_T = \cos [(\pi/3) - \gamma] \hat{e} + \sin [(\pi/3) - \gamma] \hat{p}$ ; with  $\gamma$  being a small angle ( $\sim 7 - 10^\circ$ ),  $\hat{e}$  a unit vector along the ethylene bond and  $\hat{p}$  a vector perpendicular to  $\hat{e}$  and to the *trans*-stilbene two-fold axis. The *cis*-stilbene angle is not so well known but would have the form:  $\hat{\mu}_c = \cos \alpha \hat{e} + \sin \alpha \hat{p}$ ; which is a vector perpendicular to the two-fold axis (*B* type transition) considered to be maintained during the reaction. The expected anisotropy for a process of isomerism that maintains  $C_2$  symmetry and has no overall rotation in the laboratory frame is:

$$r(t) = \frac{1}{5} \left[ 3 \cos^2 \left( \frac{\pi}{3} - \alpha - \gamma \right) - 1 \right]. \quad (9)$$

The absorption at 330 nm, assumed to be mainly *trans*-stilbene, has an anisotropy of  $0.20 \pm 0.04$  according to the most recent work (Sension *et al* 1991), implying that  $\alpha = 15 - 18^\circ$ . These results (see figure 6) are not consistent with a *cis*-stilbene transition moment nearly parallel to the ethylene bond of stilbene. The results do not easily address directly the complexity of the reaction path since the final distribution of angles is not known but suggest, as a result of the high alignment, that the reaction coordinate might involve more than simply a ring opening. The effect of solvent collisions would cause a reduction in the alignment.

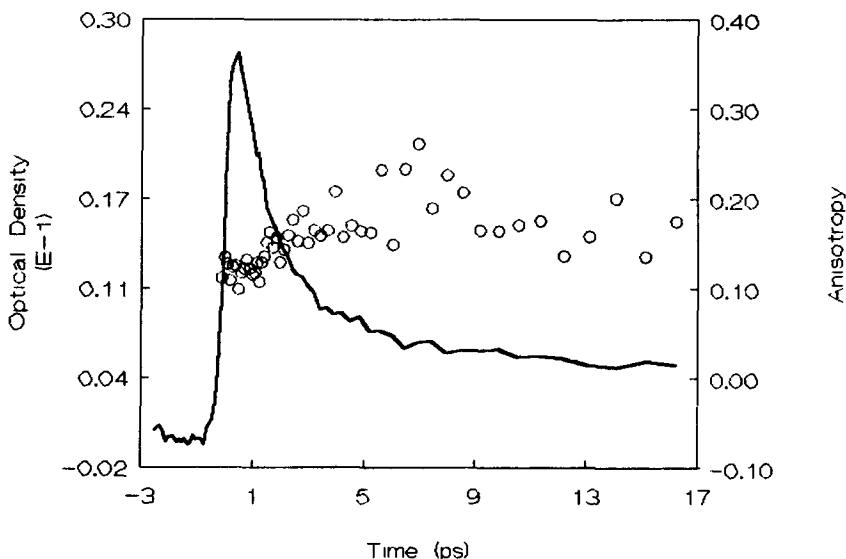


**Figure 6.** Anisotropy of the transient absorption induced by excitation of *cis*-stilbene in hexadecane, 312 nm pump, 330 nm probe. After  $\approx 5$  ps the signal is dominated by the photogenerated *trans*-stilbene.



## 6. Motions within heme proteins

Optical pump and infrared probe experiments were also used to determine structures of Fe–CO bonding in heme proteins with carbon monoxide bound to the iron of an iron protoporphyrin group (Moore *et al* 1987, 1988). Recently, ultrafast IR methods were used to discover the extent of motions of the heme region in such proteins (Lian and Locke 1991). Starting from (1) with  $\hat{\mu}_1(0)$  and  $\hat{\mu}_2(t)$  being the transition dipoles for an optical pump process involving the porphyrin and an IR probe process involving the C≡O absorption respectively, a model for the anisotropy is readily constructed. One such model is shown in figure 7. The protein is considered to be a spherical diffuser with diffusion coefficient  $D_p$  and the porphyrin is presumed to undergo small damped harmonic oscillations of angular frequency  $\omega$  about in-plane axes along and perpendicular to the plane containing the CO bond and an in-plane dielectric x-axis of the porphyrin. The anisotropy can be obtained using standard methods (Szabo 1984), assuming the two motions are uncorrelated, in the form:

$$r(t) = -\frac{1}{20} e^{-6D_p t} P_2(\cos\alpha) \left[ 1 + 3 \exp \left\{ -\frac{4k_B T}{I\omega^2} \left[ 1 - \exp \left( \frac{-\omega^2 I D t}{k_B T} \right) \right] \right\} \right], \quad (10)$$

where  $D$  is the diffusion coefficient of the porphyrin within the protein. Values of  $\omega = 3.77 \times 10^{12} \text{ S}^{-1}$  (corresponding to a  $20 \text{ cm}^{-1}$  libration),  $I = 1.1 \times 10^{-37} \text{ g cm}^2$ ,  $(6D)^{-1} = 600 \text{ ps}$  (corresponding to the rotational diffusion time for protoporphyrin-9),  $(6D_p)^{-1} = 26 \text{ ns}$  for the protein reorientation time, and an angle between the C≡O axis and porphyrin normal of  $\alpha = 18^\circ$  yield the following form for the anisotropy:

$$r(t) = -0.044 e^{-38.5t(\mu\text{s})} [1 + 3 \exp \{ -0.105(1 - e^{-0.011t(\text{ps})}) \}] \quad (11)$$

where the units for  $t$  are indicated in parentheses. Thus the  $t=0$  anisotropy is  $r(0) = -0.171$ : The value of  $\cos\alpha$  is chosen to fit the measurement at  $t=0$ . At times in excess of a few hundred ps but still very short compared with  $\mu\text{s}$  the anisotropy

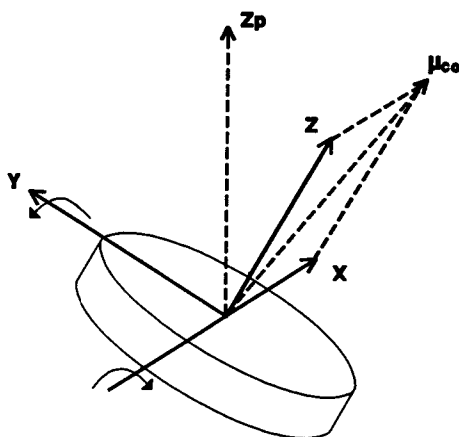


**Figure 7.** Model for calculation of IR-optical anisotropy of CO-hemoglobin. The carbonyl direction is  $\mu_{\text{co}}$ , the porphyrin axes are  $x$ ,  $y$  and  $z$  and the orientation of the whole unit in a coordinate system fixed in the protein is referred to  $Z_p$ .

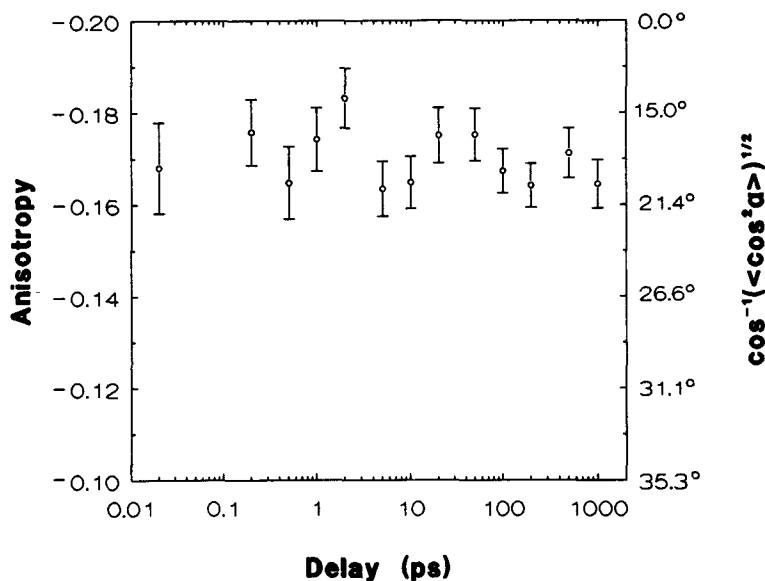


**Figure 8.** Infrared absorption anisotropy induced by polarized optical photodissociation of HbCO.

is  $-0.161$  showing an increase of  $\approx 7\%$ . The value chosen for  $\omega/2\pi c$  of  $20\text{ cm}^{-1}$  is a guess. If this were to be as high as  $\approx 70\text{ cm}^{-1}$  the fast decay part of the anisotropy would be on the  $\approx 10\text{ ps}$  timescale but the change would be much smaller. This model considers the maximal effect on the anisotropy as a result of the porphyrin undergoing motion in a harmonic potential (due to the presence of surrounding protein atoms) which is subject to a frictional damping characteristic of a porphyrin in water or glycerol (figure 8). Clearly the experiments show no significant change in  $r(t)$  with time from 300 fs to 1 ns indicating that the porphyrin is quite rigidly located in the protein as expected from X-ray diffraction in crystals. The results also indicate that the average value of  $\cos\alpha$  measured in this experiment is not influenced by motion of the sort considered here. Presumably as higher accuracy is achieved the effects of very small oscillations will become evident.

## 7. Internal rotations

Another situation can arise if a molecule can undergo quasi-free internal rotation while the whole structure is undergoing rotational diffusion. In this case unusually rapid changes in anisotropy are expected for certain orientations of the reactive transition dipoles.

The infrared anisotropy of cyclopentadienyliron dicarbonyl dimer (see figure 9) was recently studied with 580 nm excitation and 250 fs time resolution, and with 280 nm excitation and 25 ps time resolution (Iannone 1991). The change in absorbance of the antisymmetric stretch of the bridging CO groups,  $\sim 1790\text{ cm}^{-1}$ , was probed. Optical excitation leads to photodissociation of the dimer and bleaching of the IR absorption. The anisotropy obtained with 580 nm excitation in cyclohexane solvent is shown in

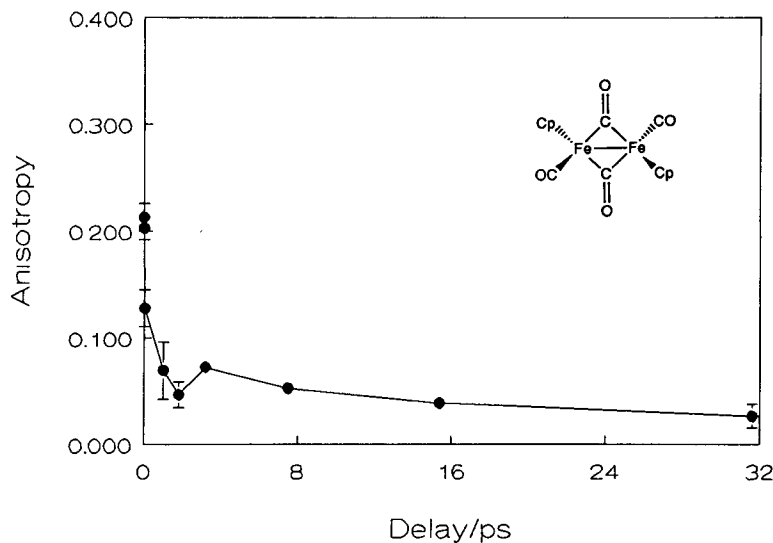


**Figure 9.** Infrared absorption anisotropy of  $\text{Fe}_2(\text{CO})_2\text{Cp}_2$  induced by polarized visible light photodissociation. Note the ultrafast ( $< 500$  fs) decay of the anisotropy.

figure 9. With 280 nm excitation and hexadecane solvent, an anisotropy of  $-0.13$  was obtained, which decays with a time constant of 50 ps. The transition dipole for the 580 nm transition is clearly parallel to the bridging CO axis while the UV transition is polarized perpendicular to this axis.

The molecule may be modelled by approximating its shape by a prolate ellipsoid. The rotational reorientation times about its three axes may then be calculated using a hydrodynamic model. Based on the results, the UV transition dipole may be assigned to the Fe–Fe axis, and a single exponential decay of the anisotropy with a time constant of 150 ps is predicted. With visible excitation a double exponential decay is predicted, with both time constants near 50 ps. The observed anisotropy with visible excitation (Iannone 1991) (see figure 9), has one component that is very fast, ca. 1 ps. Cyclopentadienyl (Cp) rings are known to rotate almost freely in Cp-metal compounds (Wilkinson and Cotton 1959) with jump rates for  $2\pi/5$  rotation on the order of  $1 \text{ ps}^{-1}$  (Altbach *et al* 1990). Thus, at least in the *trans*-isomer, rotation about an axis passing near the centers of the Cp groups could occur with little movement of the Cp. If the  $\text{Fe}_2(\text{CO})_4$  moiety were to rotate with little or no solvent friction, a fast component would be introduced into the calculated anisotropy. This may partly explain the observed behaviour of this compound.

## 8. Concluding remarks

We have shown here how the anisotropy of a pump-probe measurement is useful in exposing dynamical properties of the system that are not otherwise observable. The common feature of the examples given here is that the transition dipole responsible for the coupling of a molecule to the second (probe) photon can have a direction in space that is different from that involved in the first (pump) step. From the dynamical

viewpoint the experiment gives information about the probability distribution governing the motion of the system from one laboratory orientation to the other as a result of our knowledge of the directions of the various reactive transition dipoles in the molecular frame. Although these concepts were known for some time, the unique feature of the present study is their application to a wide variety of ultrafast phenomena in condensed phases.

### Acknowledgements

This research was supported by NSF and NIH.

### References

- Abrash S A, Repinec S T and Hochstrasser R M 1990 *J. Chem. Phys.* **90** 1041  
Altbach M I, Hiyama Y, Wittebort R J and Butler L G 1990 *Inorg. Chem.* **29** 741  
Berne B J and Pecora R 1976 *Dynamic light scattering* (New York: Wiley Inter Science)  
Gordon R G 1966 *J. Chem. Phys.* **44** 1830  
Iannone M, Diller R, Anfinrud P A, Han C, Lian T and Hochstrasser R M 1991 (to be published)  
Kim Y R, Lee M, Thorne J R G, Zeigler J M and Hochstrasser R M 1988 *Chem. Phys. Lett.* **145** 75  
Kim Y R, Share P E, Pereira M A, Sarisky M J and Hochstrasser R M 1989 *J. Chem. Phys.* **91** 7557  
Lian T and Locke R B 1991 Femtosecond transient IR study of protein internal motions in hemoglobin (to be published)  
Moore J N, Hansen P A and Hochstrasser R M 1987 *Chem. Phys. Lett.* **138** 110  
Moore J N, Hansen P A and Hochstrasser R M 1988 *Proc. Natl. Acad. Sci. USA* **85** 5062  
Motyka A, Hochstrasser R M and Topp M R 1991 Interring coupling effects in the supersonic jet spectra of bifluorene (to be published)  
Myers A B, Holt P L, Pereira M A and Hochstrasser R M 1986 *Chem. Phys. Lett.* **132** 585  
Myers A B, Pereira M A, Holt P L and Hochstrasser R M 1987 *J. Chem. Phys.* **86** 5146  
Pereira M A, Share P E, Sarisky M J and Hochstrasser R M 1991 *J. Chem. Phys.* **94** 2513  
Saltiel J and Sun Y P 1990 *Photochromism; Molecules and systems* (eds) H Bouas-Laurent and Heinz Dürr (Amsterdam: Elsevier) p. 64  
Sension R J, Repinec S T and Hochstrasser R M 1991 *J. Phys. Chem.* (in press)  
Szabo A 1984 *J. Chem. Phys.* **81** 150  
Thorne J R G, Ohsako Y, Repinec S T, Abrash S A, Zeigler J M and Hochstrasser R M 1990 *J. Lumin.* **45** 295  
Wilkinson G and Cotton F A 1959 in *Progress in inorganic chemistry* (ed.) A Cotton (New York: Interscience) vol. 1  
Wisnonski-Knittel T, Fischer G and Fischer E 1974 *J. Chem. Soc. Perkin Trans. 2* 1930